molecular pharmaceutics

pubs.acs.org/molecularpharmaceutics

Article

Bletilla striata Polysaccharide Nanoparticles Improved the Therapeutic Efficacy of Omeprazole on the Rat Gastric Ulcer Induced by Ethanol

Lisu Li,[‖] Jincheng Jing,[‖] Shanshan Yang, Shumei Fang, Wenting Liu, Cong Wang, Ruixi Li, Ting Liu, Lin Zheng, and Chang Yang*

Cite This: https://doi.org/10.1021/acs.molpharmaceut.2c00922

Read Online

ACCESS | Metrics & More | Article Recommendations

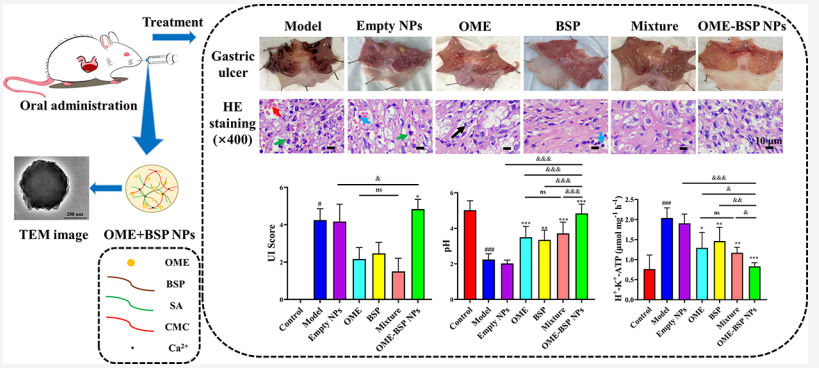

ABSTRACT: Gastric ulcers are a common clinical presentation affecting anyone, regardless of their age or gender. Nanoparticles (NPs) containing *Bletilla striata* polysaccharide (BSP) and omeprazole (OME) were investigated in the study for their therapeutic effect on gastric ulcers. Ethanol-induced gastric ulcers in rats (240 ± 30 g) were established. Our OME-BSP NPs were more stable than free OME in the acidic environment and can increase the absorption of OME in rat stomach, which was confirmed by in situ gastric absorption and distribution experiments. The extended blood circulation of OME-BSP NPs was also observed in rats with gastric ulcer. More importantly, OME-BSP NPs not only decreased the area of gastric ulcer and inhibited gastric acid secretion but also reversed gastric tissue damage and cell apoptosis, as revealed by HE and TUNEL staining. Subsequent SOD, MDA, PGE_2, IL-6, and TNF-α tests further verified the superiority of OME-BSP NPs against rat gastric ulcer, which properly originated from superior antioxidant and anti-inflammatory effects. As a result, our OME-BSP NPs' drug delivery system improved the stability and absorption of OME in the rat stomach and achieved targeted treatment of gastric ulcers.

KEYWORDS: *omeprazole, Bletilla striata polysaccharide, gastric ulcer, nanoparticles, gastric adhesion, gastric targeting*

1. INTRODUCTION

People around the world suffer from stomach ulcer disease. It is a serious health problem affecting humans.[1] Gastric ulcer is usually caused by helicobacter pylori infection,[2] alcohol consumption,[3,4] smoking,[5,6] overuse of nonsteroidal anti-inflammatory drugs (NSAIDs),[7] psychological/physiological stress,[8,9] etc. The prevalence of gastric ulcers is higher in Asian countries than in Western countries.[10,11] Oral drug therapy is the principal choice for gastric ulcer, such as antiacids,[12] proton pump inhibitors (PPIs),[13] histamine H_2 receptor antagonists,[14] etc. Since PPIs suppress gastric acid more effectively and longer, they are widely used in clinics to treat various acid-related disorders.[15] Omeprazole (OME) is the first PPI to be utilized clinically and has been in use for over 25 years.[16] Its main mechanism is to inhibit the proton pump in gastric parietal cells.[17] Since OME is activated by acidic pH to form sulfonamide intermediates, its efficacy is dependent on pH.[18] A long-term use of OME can lead to vitamin or mineral deficiency, hypergastrinemia or cardiovascular problems, as well as intestinal or respiratory infections.[19] Thus, to improve the therapeutic efficacy in the stomach, OME needs to be protected from an acidic stomach environment when taken orally.

Received: November 3, 2022
Revised: February 13, 2023
Accepted: February 16, 2023

There has been extensive use of the dried tubers of *Bletilla striata* (Thunb.) *Reichb. f.* as styptic in eastern Asian countries for centuries.[20] The excellent biocompatibility and biosafety of *B. striata* polysaccharide (BSP), a main active component of *B. striata* (Thunb.) *Reichb. f.*, have attracted much attention.[21] BSP is an acetyl glucomannan compound. Its main chain is composed of a mannose or glucose residue with a 1,2- or 1,4-link,[22,23] and its average molecular weight usually ranged from 12.6 to 235 kDa.[23,24] As the dominant active ingredient of *B. striata*, BSP can restore gastric mucosa and cure ulcers by performing anti-inflammation, suppressing the peroxidation of lipids, and enhancing local blood circulation.[20] Thus, BSP was gastroprotective. Due to its mucoadhesion, BSP was also used in the gastroretentive delivery system.[21]

To improve the stability of OME in the acidic environment and exert the synergistic effect against gastric ulcer, in this study, an inverse emulsification cross-linking method using sodium alginate (SA), carboxymethyl chitosan (CMC), and calcium ions (Ca^{2+}) was explored to load OME and BSP and obtain the OME-BSP NPs. The stability of OME-BSP NPs in the media with different pH was investigated. The absorption of OME from NPs in the stomach was studied by an in situ gastric perfusion model. The rat model with gastric ulcer induced by ethanol was established to investigate the pharmacokinetic and pharmacodynamic properties of OME-BSP NPs. A series of experiments, including gastric ulcer index, histopathological analysis, cell apoptosis assay, antioxidant and anti-inflammatory kit tests, were also carried out to confirm the therapeutic efficacy of OME-BSP NPs.

2. MATERIALS AND METHODS

2.1. Materials. Omeprazole (>98%, CAS: 73590-58-6), carboxymethyl chitosan (CMC, deacetylation degree ≥80%, CAS: 83512-85-0), urethane (>98, CAS: 51-79-6), artificial gastric juice (pH = 1.2), and artificial intestinal juice (pH = 6.8) were purchased from Yuanye Biotechnology Co., Ltd (Shanghai, China). Sodium alginate (SA, $C_6H_7NaO_6$; molecular weight: 198.11) was purchased by Chemical Reagent Co., Ltd (Shanghai, China). BSP (>98%) was obtained from Xi'an Biotechnology Co., Ltd (Xi'an, China). Calcium chloride ($CaCl_2$ >96%) was supplied by Hengxing Reagent Co., Ltd (Tianjin, China). Phosphoric acid was supplied by Sinopharm Group Chemical Reagent Company (Shanghai, China). Assay kits for hematoxylin−eosin staining (HE), TUNEL apoptosis, and 4′,6-diamidino-2-phenylindole (DAPI) were obtained from Chengdu Lilai Biotechnology Co., Ltd (Chengdu, China). Tumor necrosis factor-α (TNF-α), interleukin-6 (IL-6), and prostaglandin E2 (PGE_2) ELISA kits were supported by Shanghai Zhuocai Biotechnology Co., Ltd (Shanghai, China). H^+-K^+-ATPase activity, superoxide dismutase (SOD), and malondialdehyde (MDA) assay kits were bought from Nanjing Jiancheng Bioengineering Institute (Nanjing, China). All of our experiments were made with ultrapure water.

2.2. Preparation of OME-BSP NPs. OME-BSP NPs were prepared using an inverse emulsion and surface cross-linking method.[25,26] Briefly, Span-80 (0.36 g), paraffin oil (90 g), and OME (0.125 g) were added into a three-neck flask and stirred for 1 h at 200−300 runs per minute (rpm) as the oil phase. CMC (3.125 mg), SA (1.25 g), and BSP (0.125 g) were put into distilled water (90 mL) as the water phase. Thirty milliliters of water phase was dropped into the above oil phase (30 °C) by a pipette. The homogeneous and stable microemulsions were formed after 2 h of stirring (700 rpm). Then, 8.5 mL of $CaCl_2$ solution (15%) was incorporated into the microemulsion for the cross-linking reaction. The reaction was stirred at 30 °C at 200−300 rpm for 4 h. Finally, OME-BSP NPs were obtained by washing with hexane and ultrapure water. Their freeze-drying powder was stored at room temperature for subsequent experiments.

2.3. Characterization of OME-BSP NPs. OME-BSP NPs were characterized using a NanoBrook 90Plus PALS particle size analyzer (Brookhaven Instruments, New York). Each sample was diluted to the appropriate concentration (1:40) and transferred to a plastic cuvette for the particle size and polydispersity index (PDI) analysis at 25 °C. The samples were diluted with 10 mM NaCl solution (1:40), the surface charge (ζ-potential) of the samples was measured at 25 °C, and each cycle was performed 12 times. The particle size and surface charge of the samples were repeatedly measured three times and recorded as their mean values ± standard deviation (SD). The microstructures of OME-BSP NPs were observed under a JEOL JEM 2100 transmission electron microscope (TEM). Structural characteristics of OME-BSP NPs were analyzed by infrared spectroscopy (IRTracer-100, Shimadzu Instrument Co., Ltd. Japan, Japan) and X-ray photoelectron spectroscopy (XPS, Semmerfeld Nexsa).

2.4. OME Encapsulation Efficiency and Drug Loading of OME-BSP NPs. An appropriate amount of OME-BSP NPs was dissolved in the solution consisting of 0.01% disodium phosphate (pH = 7.4)−acetonitrile (70:30). After sonication for 30 min and centrifugation (10,000 rpm, 10 min), the OME content of solution before and after dialysis was detected by a high-performance liquid chromatography (HPLC) method, according to the 2020 edition of Chinese Pharmacopoeia. Briefly, the high-performance liquid chromatography system (Thermo Scientific UltiMate 3000, Germering, Germany) with an Agilent ZORBAX Eclipse XDB-C18 column (4.6 mm × 150 mm, 5 μm) was used. The mobile phase was 0.01% disodium phosphate (pH = 7.4)−acetonitrile (70:30) at a flow rate of 1 mL/min. OME was detected at 302 nm, and the column temperature was 40 °C. The encapsulation efficiency (EE) and drug loading (DL) were calculated according to the following equations.

$$\mathrm{EE} = \frac{M_{\mathrm{loaded}}}{M_{\mathrm{total}}} \times 100\% \quad (1)$$

$$\mathrm{DL} = \frac{M_{\mathrm{OME}}}{M_{\mathrm{NPs}}} \times 100\% \quad (2)$$

where M_{loaded} is the content of OME loaded in the nanoparticles, M_{total} is the content of OME added in the nanoparticles, M_{OME} is the weight of OME loaded in the OME-BSA NPs' freeze-dried powder, and M_{NPs} is the weight of OME-BSA NPs' freeze-dried powder.

2.5. Stability of OME-BSP NPs in the Media with Different pH. An appropriate amount of free OME or OME-BSP NPs was dispersed in 20 mL of artificial gastric juice (pH 1.2) or artificial intestinal juice (pH 6.8), and then the solutions were incubated in a water bath shaker at 37 °C for 24 h. At 0, 1, 2, 4, 8, 12, and 24 h, 1 mL of OME from different media was drawn into a centrifuge tube. The concentration of OME in the different media was detected by the above HPLC method.

https://doi.org/10.1021/acs.molpharmaceut.2c00922
Mol. Pharmaceutics XXXX, XXX, XXX−XXX

2.6. Animals. Male or female Sprague-Dawley (SD) rats (240 ± 30 g, 9−11 weeks) with certificate number SCXK (Xiang) 2019-0014 were obtained from Changsha Tianqin Biotechnology Co., Ltd (China). Rats were housed in a controlled environment (room temperature: 20 ± 5 °C, humidity: 60 ± 10%, with 12 h light−dark cycle) and fed with food and free access to water. In all animal experiments, the criteria in the Regulations on Animal Management (Document No. 55, 2001, China) of the Ministry of Health of the People's Republic of China were followed, and the Experimental Animal Ethics Committee of Guizhou Medical University approved the protocol (No. 2100881).

2.7. In Situ Gastric Absorption of OME-BSP NPs. Six rats (4 males and 2 females) were randomly divided into two groups: OME and OME-BSP NPs. Urethane solution (15%) was injected intraperitoneally. After anesthesia, the rats were fixed on an experimental table, and the abdomen was cut along the midline of the abdomen to expose the stomach. A small opening was made in the upper esophagus of the cardia and a small opening in the small intestine at the lower part of the pylorus. Then, a catheter was inserted and the openings were ligated with surgical threads. After rinsing with artificial gastric juice, the stomach was perfused with 2 mL of artificial gastric juice containing OME or OME-BSP NPs (OME: 10 mg) and put back into the abdomen. The stomach was removed after in situ absorption for 2 h, and the gastric perfusion solution was collected. The gastric parietal was repeatedly washed with artificial gastric juice. The washing fluid combined with the gastric perfusion solution was placed in a volumetric flask with a volume of 10 mL and diluted to line with artificial gastric juice. Samples were centrifuged at 12,000 rpm, and the supernatant was tested using the HPLC method described above. The calculation formula for the absorption of OME in the stomach was as follows

$$\text{Absorption (\%)} = \frac{C_0 - C_t}{C_0} \times 100\% \quad (3)$$

where C_0 is the initial concentration of OME in the artificial gastric perfusion solution and C_t is the final concentration of OME in the washing fluid combined with the gastric perfusion solution after 2 h of gastric absorption.

2.8. Establishment of Rat Model with Gastric Ulcer and Grouping. A rat model with gastric ulcer was established using the ethanol induction method described by Song et al.[27] and Jeon et al.[28] Briefly, healthy male or female SD rats (240 ± 30 g, 9−11 weeks) fasted with free access to water for 12 h. Intragastric administration of high ethanol concentration (8 mL/kg) once caused gastric mucosal erosion, gastric ulcer, and gastrointestinal bleeding.

After induction of ethanol, rats (half male and half female) were randomly divided into seven groups: Control group (normal rats + saline), model group (model rats + saline), empty NPs (model rats + empty NPs without OME and BSP), OME (model rats + OME, OME: 18 mg/kg), BSP (model rats + BSP, BSP: 0.68 mg/kg), mixture (model rats + OME + BSP, OME: 18 mg/kg; BSP: 0.68 mg/kg), and OME-BSP NPs (model rats + OME-BSP NPs, OME: 18 mg/kg; BSP: 0.68 mg/kg). The samples were administered intragastrically once a day for 3 days.

2.9. Ultra High-Performance Liquid Chromatography-Tandem Mass Spectrometry (UPLC-MS/MS) Analysis of OME. The UPLC-MS/MS method for OME detection was performed using the Waters Xevo TQ MS system (Waters, Milford, MA). MassLynxV 4.1 software was used for system operation. The chromatographic separation was using an ACQUITY UPLC BEH C18 column (2.1 mm × 50 mm, 1.7 μm), and the mobile phase consisted of 2% formic acid water solution (A) and 2% formic acid−acetonitrile solution (B). The gradient elution procedure was as follows: 0.0−0.5 min, 90% A−90% A and 10% B−10% B; 0.5−3.5 min, 35% A−35% A and 65% B−65% B; 3.5−4.5 min, 10% A−10% A and 90% B−90% B; 4.5−5 min, 90% A−90% A and 10% B−10% B. The flow rate was 0.35 mL/min; the column temperature was 40 °C; and the injection volume was 1 μL. The OME assay was performed in the positive ionization and multiple reaction monitoring (MRM) mode. OME and puerarin were quantified using the parent ion, m/z 346.10 for OME, and 417 for puerarin. The daughter ions were m/z 198.10 (OME) and m/z 267 (puerarin). The optimized parameters for OME determination were as follows: capillary ionization voltage at 2.5 kV; collision energy at 35 V; cone voltage at 30 V for OME and 40 V for puerarin; ion source temperature at 600 °C; spray gas and blow gas were nitrogen; the desolvation gas temperature at 350 °C; and the desolvation gas flow rate at 1000 L/h.

2.10. Sampling. After the last treatment, blood was taken from the rat's crotch artery and placed in a plastic tube containing 1% heparin. Blood was collected and placed at room temperature for 1−2 h. After centrifugation (4 °C/3500 rpm/10 min), serum was then separated for further use. The rat stomach was removed, and the gastric contents were collected into a 30 mL centrifuge tube by cutting the specimen along the greater curvature. The contents were centrifuged (4 °C/3500 rpm/10 min), and the supernatant was separated for later analysis. And the gastric tissue was washed with cold saline and photographed. Then, the gastric tissue was divided into two parts: one part was stored in 10% neutral formalin for histological analysis and the other part was prepared as a 10% tissue homogenate for kit analysis.

2.11. Pharmacokinetic Study. Thirty-six rats with gastric ulcer (half male and half female) were divided into three groups randomly: OME (OME: 18 mg/kg), mixture (OME: 18 mg/kg; BSP: 0.68 mg/kg), and OME-BSP NPs (OME: 18 mg/kg; BSP: 0.68 mg/kg). The sample was dosed orally one time. The rat blood samples (0.25 mL) from their orbits were collected at 0.5, 0.75, 1, 1.5, 2, 3, 4, 6, 8, 10, 12, and 24 h after the treatment and placed into a centrifuge tube containing 1% heparin. After centrifugation (4 °C/3500 rpm/10 min), the supernatant (100 μL), puerarin in methanol (30.01 ng/mL, 50 μL) as the internal standard, 1% formic acid solution (50 μL), and methanol (400 μL) were added in order into a centrifuge tube, sonicated (10 min), and mixed (2 min). Under a nitrogen gas flow at 37 °C, the supernatant (500 μL) from centrifugation (4 °C/12,000 rpm/10 min) was dried. The residue was reconstituted in 200 μL of 50% methanol and centrifuged (4 °C/12,000 rpm/10 min). A sampler vial was filled with the supernatant, and 1 μL was subsequently injected for UPLC-MS/MS analysis.

2.12. Distribution of OME in the Stomach and Intestine. Twelve rats (half male and half female) with gastric ulcer were randomly divided into two groups: OME (OME: 18 mg/kg) and OME-BSP NPs (OME: 18 mg/kg; BSP: 0.68 mg/kg). The samples were administered intragastrically one time. Rats were killed by cervical dislocation at 2 and 10 h. The stomach and intestine were quickly taken and

https://doi.org/10.1021/acs.molpharmaceut.2c00922
Mol. Pharmaceutics XXXX, XXX, XXX−XXX

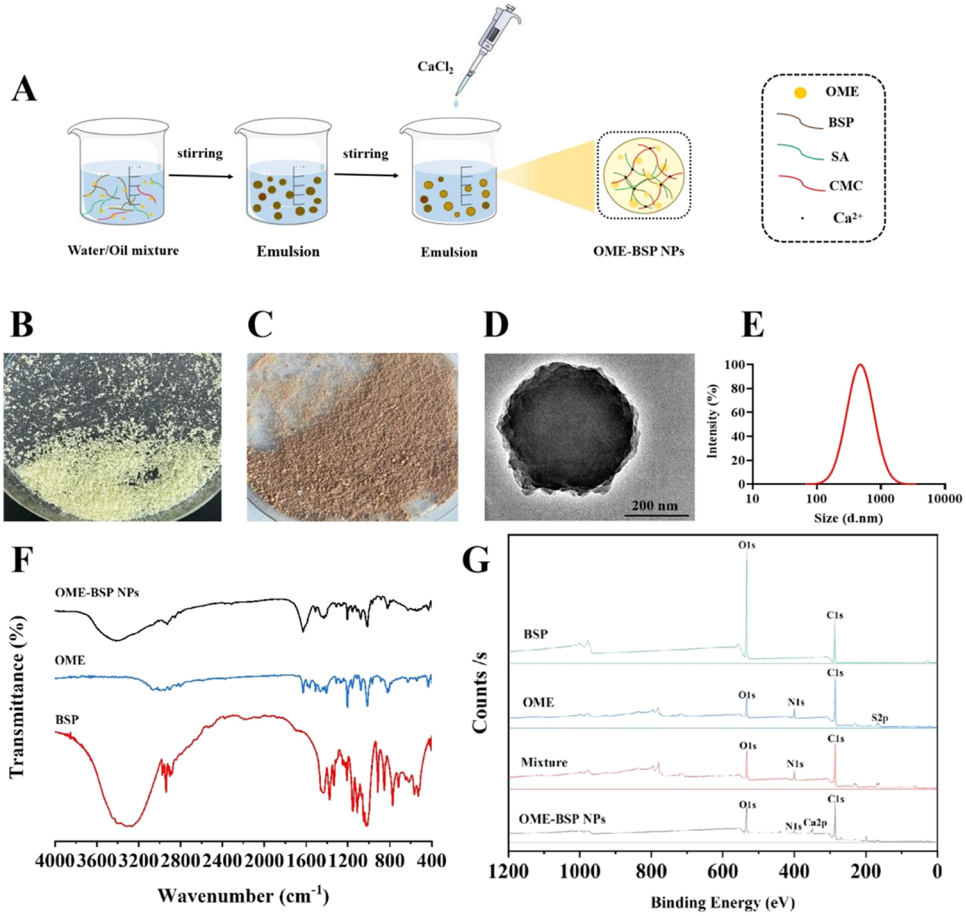

Figure 1. Scheme of OME-BSP NP preparation and characterization of OME-BSP NPs. (A) Scheme of OME-BSP NP preparation by the emulsion cross-linking method. (B) Image of empty NP powder. (C) Image of OME-BSP NPs. (D) TEM images of OME-BSP NPs. (E) Hydrodynamic diameter measured by the NanoBrook 90Plus PALS particle size analyzer (Brookhaven Instruments, New York). (F) Infrared spectra of BSP, OME, and OME-BSP NPs. (G) XPS spectra of BSP, OME, mixture, and OME-BSP NPs.

homogenized with saline. The procedure described in Section 2.11 was followed for pretreatment and analysis of each sample of tissue homogenate.

2.13. Gastric Ulcer Score. To assess ulcer formation, stomachs were unclosed along the greater curvature and rinsed with water to remove gastric contents and blood clots. Ulcers were counted and scored by the method as described earlier.[29] The specific scoring criteria were as follows: normal colored stomach (0), red coloration (0.5), spot ulcer (1), hemorrhagic streak (1.5), deep ulcers (2), and perforation (3). The gastric ulcer was scored as average gastric ulcer in each group of rats.

2.14. Estimation of pH and the Activity of H^+-K^+-ATPase in Gastric Secretion. According to the procedure described in Section 2.10, the gastric contents and stomach tissues of rats in each group were taken. The pH from the supernatant of gastric contents was determined by a pH meter (Shanghai BANTE instruments co., Ltd., China), and the activity of gastric H^+-K^+-ATPase was determined from 10% gastric tissue homogenate, according to the introduction of H^+-K^+-ATPase activity assay kit (Zhucai Biotechnology Co., Ltd. Shanghai, China), by a microplate reader (Variosska, Semmerfeld Nexsa) at 660 nm.

2.15. Hematoxylin and Eosin (H&E) Staining. Gastric tissue was collected from each group by the procedure described in Section 2.10. A routine process of tissues was consistent as described in the study.[30] After that, morphological changes of gastric mucosa in rats were observed and imaged under an optical microscope (BA210Digital, Mac Audi Industrial Group Co., Ltd. China).

2.16. TUNEL Assay. Following the procedure outlined in Section 2.10, each group of gastric tissue was collected. Based on the manufacturer's instructions, gastric tissue was stained with an FITC-labeled TUNEL kit and restained with DAPI solution. Using a panoramic slide scanner (3DHISTECH, Hungary), the colored slides were scanned. DAPI stained normal cells blue, and FITC stained apoptotic cells green. UV excitation wavelengths of DAPI and FITC were 377 and 492 nm, respectively, and their emission wavelengths were 447 and 506 nm. Following was the formula for calculating positive apoptosis rate (%)

$$\text{Positive apoptosis rate} = \frac{\text{number of positive cells}}{\text{number of total cells}} \times 100\% \quad (4)$$

2.17. Biochemical Analysis in Serum. Six rats with gastric ulcer (half male and half female) in each group were dosed for three consecutive days, and then the blood samples were collected from their orbits and placed at room temperature for 1−2 h. After blood stratification, the samples were centrifuged at 3500 rpm and 4 °C for 10 min. Serum was separated for further use. According to the manufacturer's introductions, SOD and MDA levels were determined by the

https://doi.org/10.1021/acs.molpharmaceut.2c00922
Mol. Pharmaceutics XXXX, XXX, XXX−XXX

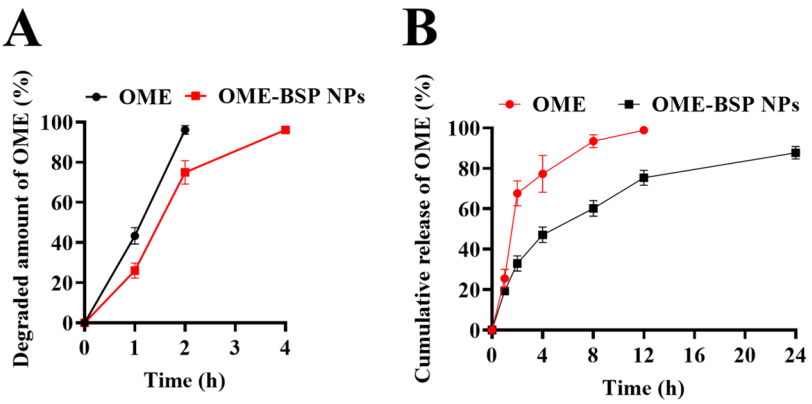

Figure 2. Stability of OME and OME-BSP NPs in artificial gastric juice and the release profile in artificial intestine juice. (A) Degradation curve of OME and OME-BSP NPs in artificial gastric fluid (pH = 1.2) from 0 to 4 h (n = 3). (B) Cumulative release curve of OME and OME-BSP NPs in artificial intestinal fluid (pH = 6.8) from 0 to 24 h (n = 3).

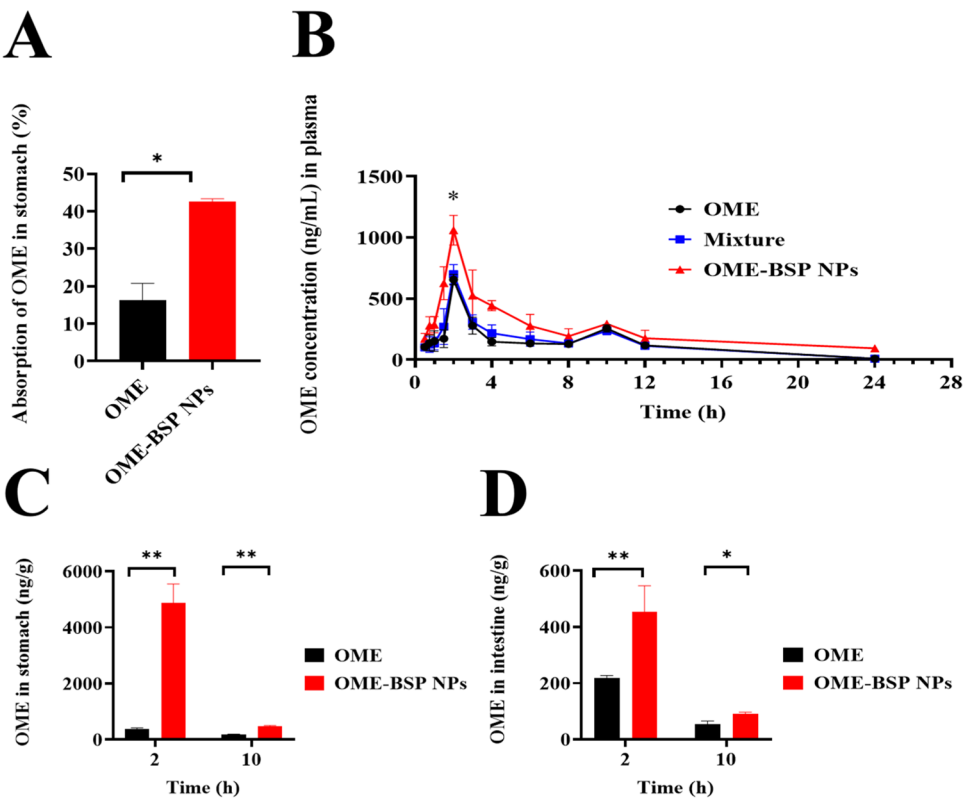

Figure 3. Gastric absorption and levels of OME in blood, stomach, and intestine. (A) Absorption of OME and OME-BSP NPs in situ gastric perfusion for 2 h. (B) Plasma concentration of OME versus time profile. (C) Distribution of OME in the stomach at 2 and 10 h. (D) Distribution of OME in the intestine at 2 and 10 h. Data were presented as the mean ± SD (n = 3), *P < 0.05 or **P < 0.01 vs OME.

spectrophotometers, and PGE2, IL-6, and TNF-α levels were measured by the ELISA method.

2.18. Statistical Analysis. The stability of OME-BSP NPs and in situ gastric absorption were analyzed by independent-sample t-test. WinNonLin 8.2 software calculated pharmacokinetic parameters and their differences were analyzed by one-way analysis of variance (ANOVA). An analysis of the gastric ulcer score was performed using the Kruskal–Wallis nonparametric test (K–W test). Two-tailed t-test was used in the analysis of gastric pH and the gastric cell apoptosis rate. The H^+-K^+-ATPase activity, MDA, SOD, PGE_2, IL-6, and TNF-α were analyzed via one-way analysis of variance (ANOVA), followed by the LSD or Dunnett T3 testing. The data were analyzed by SPSS 26.0 to determine mean and standard deviation of at least three independent experiments. The level of significance was set at P < 0.05.

3. RESULTS

3.1. Preparation and Characterization of the OME-BSP NPs. OME-BSP NPs were prepared by the inverse emulsification cross-linking method (Figure 1A). The obtained powder of empty NPs (Figure 1B) was yellow. After being loaded with OME and BSP, the powder of OME-BSP NPs (Figure 1C) was brown. Observed under the transmission electron microscope (TEM) (Figure 1D), OME-BSP NPs were spherical with diameters ranging from 181 to 455 nm. By

https://doi.org/10.1021/acs.molpharmaceut.2c00922
Mol. Pharmaceutics XXXX, XXX, XXX−XXX

Table 1. Pharmacokinetic Parameters[ab]

parameters	units	OME	mixture	OME-BSP NPs
$t_{1/2}$	h	2.88 ± 0.32	2.93 ± 0.20	9.40 ± 1.00**
C_{max}	ng/mL	655.15 ± 42.56	699.20 ± 78.99	1059.19 ± 121.19**
AUC	h×ng /mL	3101.44 ± 261.30	3423.11 ± 29.88	6045.85 ± 156.06**
$AUC_{0-\infty}$	h×ng /mL	3134.49 ± 271.45	3457.39 ± 327.54	7312.49 ± 298.28**
V_z	L/h/kg	23.86 ± 2.11	22.20 ± 3.00	33.35 ± 2.15**
Cl_z	L/kg	5.77 ± 0.51	5.24 ± 0.50	2.46 ± 0.10**
$MRT_{0-\infty}$	h	7.50 ± 0.08	7.31 ± 0.32	13.08 ± 0.45**

[a]Data are shown as mean ± SD (n = 3). **P < 0.01 vs OME group. [b]$t_{1/2}$, terminal elimination half-life; AUC, area under the plasma concentration versus time curve from zero to the last sampling time; $AUC_{0-\infty}$, area under the plasma concentration versus time curve from zero to infinity; Cl_Z, total body clearance; V_z, apparent volume of distribution; $MRT_{0-\infty}$, mean retention time from zero to infinity.

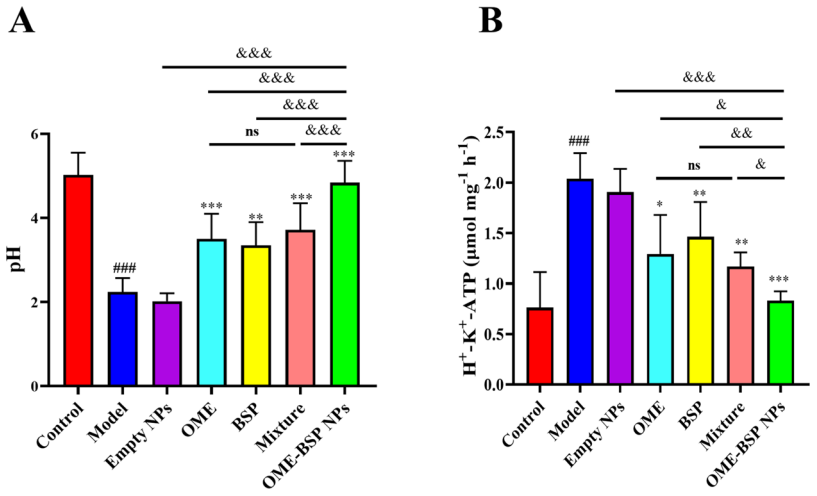

Figure 4. OME-BSP NPs can suppress gastric acid secretion in gastric ulcer rats through inhibiting the H^+-K^+-ATPase activity. (A) The pH value of gastric contents. (B) H^+-K^+-ATPase activity in the stomach. Data were presented as the mean ± SD (n = 6). ###P < 0.001 vs control; **P < 0.01, ***P < 0.001 vs model; &P < 0.05, &&P < 0.01, &&&P < 0.01 vs OME-BSP NPs; ns indicated no statistical difference, P > 0.05.

measuring with the NanoBrook 90Plus PALS particle size analyzer, their hydrodynamic diameter was around 380 nm (Figure 1E), PDI was 0.24 ± 0.01, and the negative surface charge (ζ-potential) was −18.81 ± 1.05 mV. The OME EE of OME-BSP NPs was 77.20 ± 13.95%, and DL was 30.28 ± 5.04%. According to their infrared spectra (Figure 1F), BSP and OME-BSP NPs exhibited −OH stretching vibration of polysaccharide around 3300 cm^{-1} and the weak bands around 2980 cm^{-1} representing the C−H stretching vibration of $-CH_2$.[31] Both OME and OME-BSP NPs showed similar IR spectra below 2400 cm^{-1}. The possible reason was that the molecular ratio of OME was higher than that of BSP since the weight ratio of their addition was 1:1. It was confirmed by these results that NPs were successfully loaded with BSP and OME, as well as by XPS spectra (Figure 1G). C 1s, O 1s, and N 1s atoms had no obvious peak shift in BSP, OME, mixture, and OME-BSP NP groups. Due to the content of S atoms lower than 5% in the nanoparticles, the S 2p atoms in OME were missing in OME-BSP NPs. The appearance of Ca 2p atoms in the OME-BSP NPs implied the successful cross-linking caused by the introduction of $CaCl_2$.

3.2. OME-BSP NPs Can Improve the Stability of OME In Vitro. The degradation curve of OME and OME-BSP NPs in artificial gastric juice (pH 1.2) and the release curve in artificial intestinal juice (pH 6.8) were investigated to evaluate the stability of OME-BSP NPs. As illustrated in Figure 2A, in the acid environment (pH 1.2), the degradation amount of free OME at 2 h was 96.12 ± 2.15%, which implied that it was completely destroyed. However, the OME degradation amount in the OME-BSP NPs at 2 and 4 h was 74.92 ± 5.84 and 96.13 ± 0.27%, respectively. As shown in Figure 2B, OME was relatively stable in the artificial intestinal juice (pH.6.8). Free OME released 98.89 ± 1.55% at 12 h, while OME-BSP NPs can continuously and stably release OME in the media of pH = 6.8 for up to 24 h, and the cumulative release amount at 24 h was 87.70 ± 3.09%. In summary, BSP NPs can improve the stability of OME in the artificial gastric fluid and achieve the sustained release of OME in artificial intestinal fluid.

3.3. OME-BSP NPs Can Increase the In Situ Gastric Absorption of OME. Considering the periodic motion of rat stomach,[32] in situ gastric absorption of OME and OME-BSP NPs was investigated at 2 h. In Figure 3A, the gastric absorption of free OME (16.30 ± 4.45%) was much less than that of OME-BSP NPs (42.57 ± 0.78%), and OME-BSP NPs can enhance the absorption of OME in the stomach of rats.

3.4. OME-BSP NPs Increased the OME Level in the Blood, Stomach, and Intestine of Rats with Gastric Ulcer. The mean plasma concentration−time profiles of OME, mixture, and OME-BSP NPs in the model rats are shown in Figure 3B, and the pharmacokinetic parameters of OME were obtained by WinNonLin 8.2 software (Table 1). As depicted in Figure 3B and Table 1, similar pharmacokinetic parameters of OME in the free OME group and the mixture group were observed without a significant difference, indicating that simple physical mixing cannot influence the pharmacokinetics of OME. However, the AUC of OME in the OME-BSP NPs had

https://doi.org/10.1021/acs.molpharmaceut.2c00922
Mol. Pharmaceutics XXXX, XXX, XXX−XXX

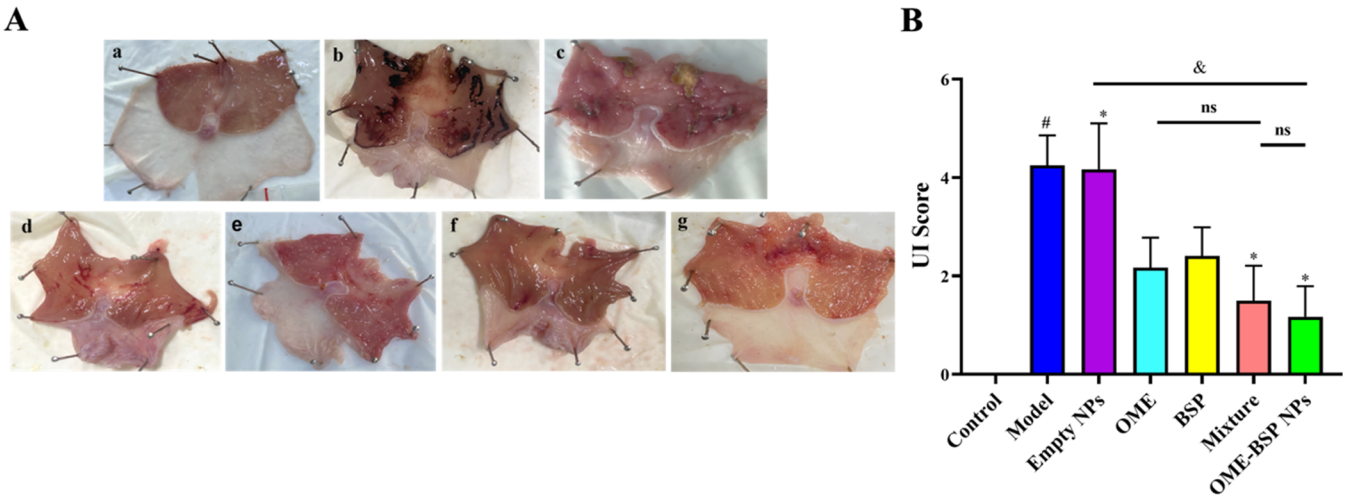

Figure 5. Typical pictures (A) and the score (B) of gastric ulcers in each group of rats. (A) Typical pictures of gastric ulcers in each group of rats. a: Control, b: Model, c: Empty NPs, d: OME, e: BSP, f: Mixture, g: OME-BSP NPs. (B) Gastric ulcer score in each group of rats. Data are presented as average ± SD (n = 6). $^{###}P < 0.001$ vs control; $^{*}P < 0.05$,$^{**}P < 0.05$ vs model; ns indicated no statistical difference, $P > 0.05$.

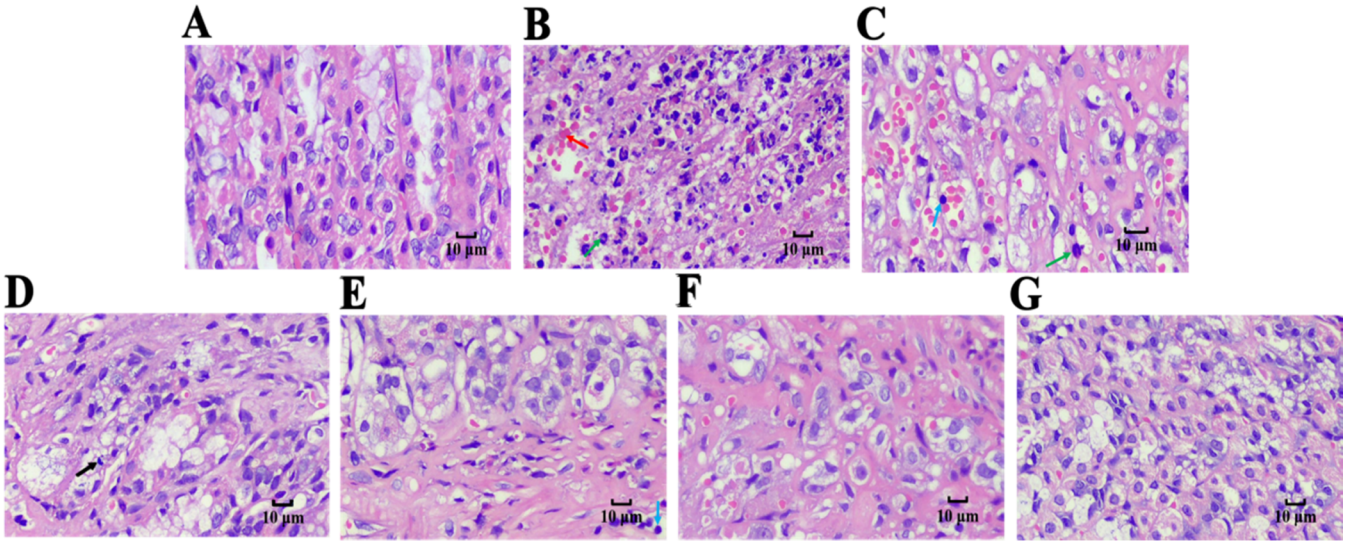

Figure 6. Typical images of H&E-stained gastric tissue (scale bar: 10 μm) in rats after OME, BSP, mixture, and OME-BSP NP treatments (n = 6). Mucosal gastric gland necrosis (↑), neutrophils (↑), bleeding (↑), lymphocytes (↑). A: Control group; B: Model group; C: Empty NPs; D: OME group; E: BSP group; F: Mixture group; G: OME-BSP NP group.

a 2-fold increase ($P < 0.01$) from 0.5 to 24 h compared with free OME (6045.85 ± 156.06 vs 3101.44 ± 261.30 h×ng/mL) revealed in Table 1, indicating that OME-BSP NPs had higher OME concentration (C_{max}: 1059.19 ± 121.19 vs 655.15 ± 42.56 ng/mL) in the systemic circulation ($P < 0.01$) and a 3-fold extended half-life time ($t_{1/2}$: 9.40 ± 1.00 vs 2.88 ± 0.32 h, $P < 0.05$). Correspondingly, the V_z of OME in the OME-BSP NP group increased (V_z: 33.35 ± 2.15 vs 23.86 ± 2.11 L/h/kg) and the CL_z values of OME in the OME-BSP NP group decreased (CL_z: 2.46 ± 0.10 vs 5.77 ± 0.51 L/kg).

Similar to the OME plasma level, the level of OME both in the rat stomach and intestine increased ($P < 0.01$) at 2 and 10 h after NP encapsulation (Figure 3C,D). Especially, at 2 h, the level of OME from OME-BSP NPs in the stomach reached 4870 ± 683.44 ng/g and in the intestine was 453.29 ± 93.66 ng/g, while the level of OME from free OME group in the stomach was 388.46 ± 27.12 ng/g and in the intestine was 217.64 ± 9.59 ng/g. These results further verified that BSP NP encapsulation can increase the absorption of OME in the stomach, which was also found in the in situ gastric perfusion absorption experiment.

3.5. OME-BSP NPs Can Suppress the Secretion of Gastric Acid through Inhibiting the Activity of H^+-K^+-ATPase. Suppression of acid production can improve gastric ulcer.[13] As observed in Figure 4A, the pH value of normal rats was 4.84 ± 0.52, while the pH value of model rats was 2.24 ± 0.33 ($P < 0.001$). The pH of rat stomach in the OME-BSP NP group was significantly higher than that of empty NPs, OME, BSP, and mixture ($P < 0.001$) and nearly recovered to that of normal rats, implying the superior therapeutic efficacy over OME and BSP alone against gastric ulcer. As well known, OME can greatly inhibit the activity of the H^+-K^+ ATPase enzyme, resulting in the suppression of gastric acid secretion (Figure 4B), as reported in other literature studies.[8,33] Interestingly, OME-BSP NPs had a better inhibition of H^+-K^+-ATP enzymes, reduced the release of H^+, protected the gastric mucosa, and finally reduced ulcer formation (Figure 5).

https://doi.org/10.1021/acs.molpharmaceut.2c00922
Mol. Pharmaceutics XXXX, XXX, XXX−XXX

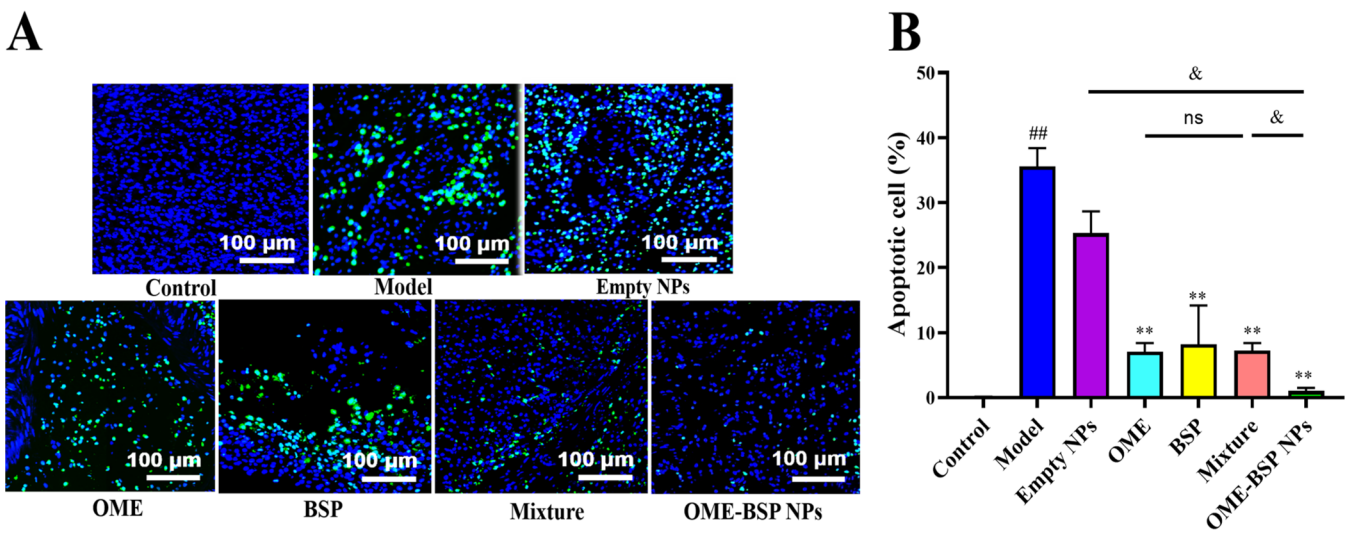

Figure 7. Apoptosis of gastric cells after OME, BSP, mixture, and OME-BSP NP treatments. (A) Typical images of gastric cells (scale bar: 100 μm) stained with TUNEL. (B) Percentage of apoptotic cells in the stomach of gastric ulcer rats. Data were presented as the mean ± SD (n = 3). $^{\#\#}P$ < 0.01 vs control. $^{*}P$ < 0.05; $^{**}P$ < 0.01 vs model; $^{\&}P$ < 0.05 vs OME-BSP NPs; ns indicated no statistical difference, P > 0.05.

3.6. OME-BSP NPs Can Recover the Rat Gastric Ulcer. An imbalance between destructive factors and mucosal defense mechanisms in the mucosal epithelium causes gastric ulcer.[34] In Figure 5A, the normal rats in the control group had no obvious bleeding, and their gastric mucosa was thick and pale pink. The rats with gastric ulcer induced by ethanol in the model group had a mass of black cord-like ulcers, and the ulcers ran through the entire gastric mucosa. Compared with normal rats in the control groups, the gastric mucosa of model rats was loose, thin, and seriously damaged, which confirmed that the rat gastric ulcer model was successfully established. When rats were treated with OME, BSP, mixture, or OME-BSP NP group, the surface of gastric mucosa was smooth and wrinkled with only a few bleeding points. In Figure 5B, the gastric ulcer score of rats in the model group and empty NP group were 4.25 ± 0.61 and 4.17 ± 0.93, respectively. After treatments with OME, BSP, mixture, and OME-BSP NPs, the gastric ulcer score decreased to 2.17 ± 0.61, 2.41 ± 0.58, 1.50 ± 0.71, and 1.17 ± 0.62, respectively. These results further verified that OME-BSP NPs indeed can treat gastric ulcer and their therapeutic efficacy was superior to OME or BSP alone.

3.7. OME-BSP NPs Can Reverse the Histopathological Change in the Stomach. Histopathological changes in the stomach were revealed by H&E staining (Figure 6). The normal gastric mucosa was complete, and the mucosal layer was covered with a single layer of columnar epithelium. There was no obvious hyperplasia in the gastric mucosa with no inflammatory cell infiltration in the muscularis and adventitia, while broken mucosa with severe hemorrhage (red arrow) and inflammatory cell infiltration (green arrow) appeared in the H&E-stained stomach tissues induced by ethanol in the model group as previously reported by other studies.[35,36] Empty NPs did not exhibit any noticeable improvement in pathological tissue, with hemorrhage, neutrophils (green arrows), and lymphocytes (blue arrows) still present. In the OME group, the gastric tissue was also damaged with superficial degeneration, necrosis of the mucosal layer in some areas (black arrow), and loose connective tissue. In the BSP group, the connective structure of tissue was loose with the lymphocyte infiltration (blue arrow). Similar to the histological change observed in the OME group, the gastric tissue was slightly damaged, and there was no obvious edema and inflammatory cell infiltration. As for OME-BSP NP groups, the structure of gastric mucosa, submucosa, muscular layer, and serosa was relatively complete, and a small number of lymphocytes were scattered occasionally without obvious pathological changes. In summary, OME-BSP NPs can reverse the histological change of gastric tissue induced by ethanol, and their therapeutic efficacy was the best.

3.8. OME-BSP NPs Can Alleviate the Cell Apoptosis Induced by Ethanol. Apoptosis is a genetically determined energy-dependent process and a homeostatic mechanism that maintains cell populations in tissues.[37] However, gastric ulcers often lead to imbalances in energy and homeostasis. Thus, apoptosis in gastric tissues was investigated by TUNEL staining (Figure 7A). Apoptotic cells were stained with FITC and normal cells with DAPI. As described in Figure 7B, the normal gastric tissue in the control group had few apoptotic cells (0.11 ± 0.04%), while a substantial number of apoptotic cells were seen in TUNEL-stained gastric sections of the model group (35.57 ± 2.82%). After administered with OME (7.02 ± 1.36%), BSP (8.17 ± 5.99%), mixture (7.21 ± 1.18%), and OME-BSP NPs (1.01 ± 0.49%), the apoptotic cells significantly decreased compared to that in the model group (P < 0.01), and this change was pronounced in the OME-BSP NP group (P < 0.05). Consistent with the interesting findings above, OME-BSP NPs provide greater protection against gastric injury than OME or BSP alone at an equivalent dose.

3.9. OME-BSP NPs Can Improve the Gastric Ulcer through Antioxidant and Anti-inflammatory Pathways. Exogenous and endogenous production of reactive oxygen species and free radicals predispose to mucosal damage,[38,39] which in turn leads to the formation of gastric ulcers. The role of SOD is to convert superoxide produced during oxidative stress into hydrogen peroxide.[40,41] MDA is produced by the peroxidation of polyunsaturated fatty acids or related esters in the cell membrane.[42] This transition to an oxidative state is caused by the release of hydroperoxide radicals and superoxide anions, and their increase leads to oxidative stress, which can be seen as an increase in MDA levels.[43] In this study, oral

https://doi.org/10.1021/acs.molpharmaceut.2c00922
Mol. Pharmaceutics XXXX, XXX, XXX−XXX

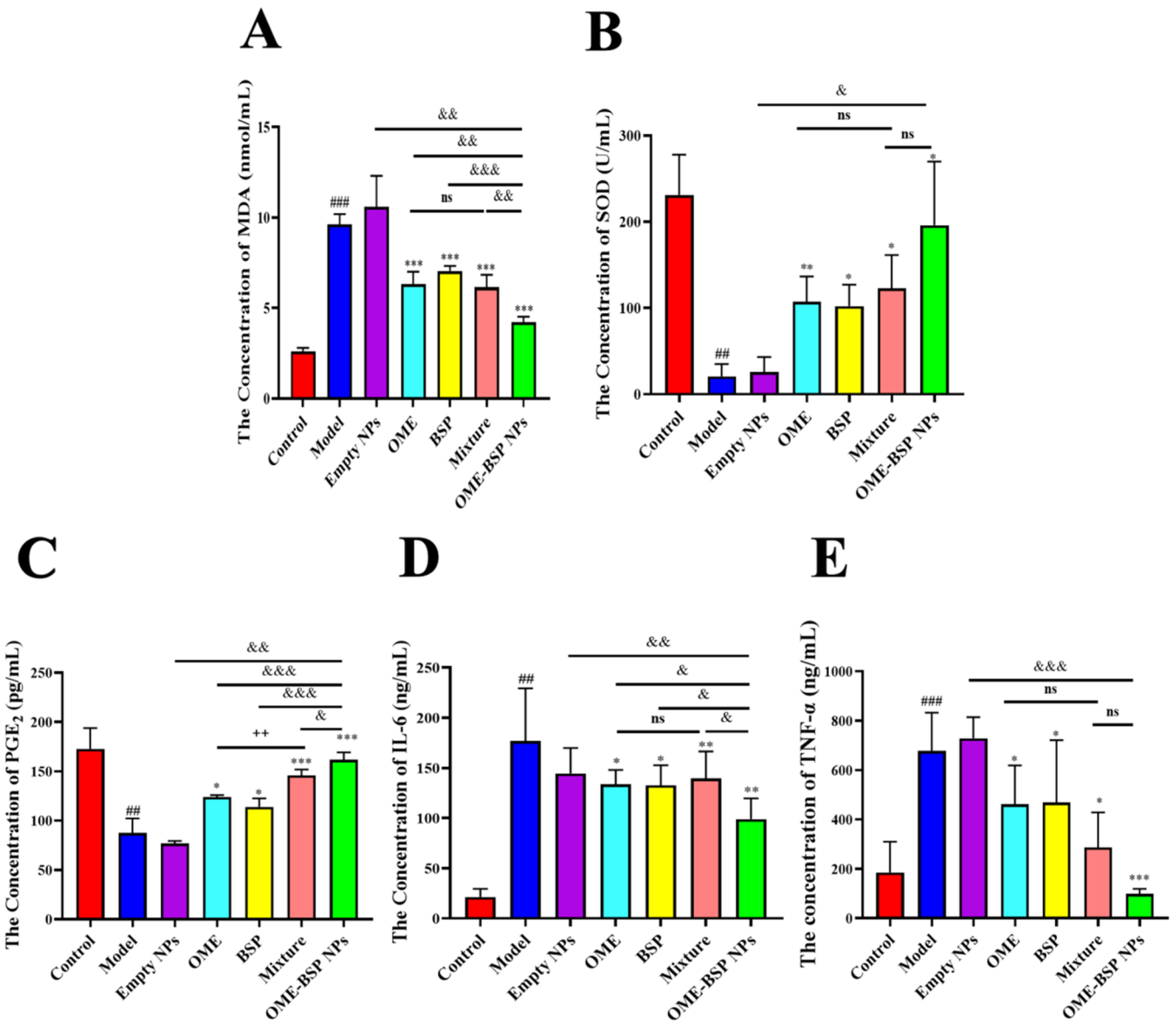

Figure 8. OME-BSP NPs reduced the oxidative stress and inflammation levels in rats with gastric ulcer. (A) MDA activity in the serum. (B) SOD content in the serum. (C) PGE_2 content in the serum. (D) IL-6 level in the serum. (E) TNF-α level in the serum. Data were presented as the mean ± SD ($n = 6$). $^{\#}P < 0.05$, $^{\#\#}P < 0.01$, $^{\#\#\#}P < 0.001$ vs control. $^{*}P < 0.05$, $^{**}P < 0.01$ vs model. $^{++}P < 0.01$ vs OME. $^{\&}P < 0.05$, $^{\&\&}P < 0.01$, $^{\&\&\&}P < 0.001$ vs OME-BSP NPs; ns indicated no statistical difference, $P > 0.05$.

alcohol markedly increased MDA levels and reduced SOD activity (Figure 8A and B), supporting the notion that oxidative stress plays an essential role in the pathogenesis of alcohol-induced gastric injury.[9] Interestingly, OME, BSP, mixture, and OME-BSP NPs can decrease the MDA levels and increase the SOD activity to some extent, and OME-BSP NPs were more effective on the antioxidative activities than physical mixtures of OME and BSP during the MDA test ($P < 0.01$).

The inflammatory response was activated when gastric mucosa was damaged, and it may cause secondary mucosal damage.[44] Prostaglandins (PGs) produced by gastric mucosal cells were important endogenous mediators of acute gastric mucosal injury.[45] Therefore, PGE_2 plays an important role in gastric ulcer healing. The effect of OME-BSP NPs on ethanol-induced gastric PGE_2 levels in rats using ELISA kits was determined to measure PGE_2 content. In comparison with the model group, the PGE_2 content increased in the BSP, OME, mixture, and OME-BSP NP groups (Figure 8C) and reached the highest point in OME-BSP NPs ($P < 0.01$). In addition, the content of PGE2 in the mixture group was higher than that in the OME group ($P < 0.001$). The serum levels of inflammatory factors in each group were also investigated (Figure 8D and E). As shown in the model group, the levels of IL-6 and TNF-α were notably increased in rats after gastric exposure to ethanol. Undoubtedly, OME-BSP NPs displayed better anti-inflammatory properties than OME or BSP alone ($P < 0.05$), even better than their physical mixture ($P < 0.05$), and OME-BSP NPs properly had the synergistic antioxidant and anti-inflammatory effects against gastric ulcer.

4. DISCUSSION

Gastric ulcer is a chronic condition with unexpected complications, including bleeding, stenosis and perforation,

https://doi.org/10.1021/acs.molpharmaceut.2c00922
Mol. Pharmaceutics XXXX, XXX, XXX−XXX

and a high recurrence rate.[8] An imbalance between destructive factors and mucosal defense mechanisms in the mucosal epithelium causes gastric ulcer.[34] Proton pump inhibitors such as OME have been found to increase the healing and improve clinical symptoms of gastric ulcer.[46] However, the instability of OME in the acid environment limited their therapeutic efficacy. Thus, their enteric-coated capsules were developed to solve this problem. To improve the stability of OME in the stomach and increase the gastric targeting, BSP was chosen to construct a mucoadhesive drug delivery system in our study because of their biodegradability, biocompatibility, low cost, and high security.[47] More importantly, BSP also could exert antiulcer activity by inhibiting lipid peroxidation reaction, improving local blood circulation in ulcer lesions and promoting repair of the gastric mucosa through adherence to the gastric mucosa.[31,48−52] As a result, we designed this mucodrug delivery system to treat gastric ulcer using SA and CMC to load OME and BSP.

As far as we know, this is the first study to combine OME with BSP in the nanoparticles to treat rat gastric ulcers. As shown in Figures 2 and 3, OME-BSP NPs can increase the stability of OME in the acid environment both *in vitro* and *in vivo*, resulting in the extension of OME half-life time (Table 1) and the absorption of OME in the rat stomach (Figure 3A and C). Finally, the area of gastric ulcer decreased, the histological change was reversed, apoptotic cells in gastric tissue decreased, and oxidant stress and inflammation were relieved after treatments with OME, BSP, mixture, and OME-BSP NPs as shown in Figures 4−8. As expected, the therapeutic efficacy of OME-BSP NPs was superior to that of OME or BSP alone, even better than their physical mixture. There were perhaps four reasons behind this fact. First, BSP is a dual-use material. On the one hand, BSP can treat gastric ulcer by repairing the gastric mucosa, hemostasis,[31] and inhibiting inflammation.[53−56] On the other hand, BSP is a bioadhesive material. Under the acid environment, BSP may form the gel, increase the adhesion, and form a protective membrane on the gastric mucosa.[57] The gastric acid stopped eroding the ulcer area, and the membrane of BSP increased the accumulation of OME at the ulcer area.[58] Even in the lesion site, OME was directly activated to treat the ulcer. Second, nanoparticles were more readily ingested by immune-associated cells, namely, macrophages in areas of active inflammation.[59−61] Thus, BSP NPs can inhibit inflammation as soon as possible. Third, in nanoparticles, the mixed state of OME and BSP was more uniform and closer together than the mixture alone. Although no chemical bonding existed between OME and BSP, OME and BSP were wrapped in the network structure formed by cross-linked SA in proportion. The combination of BSP and OME in the nanoparticles can play a better synergistic effect, which was observed in the pharmacodynamic tests (Figures 4−8). Finally, but not the last, OME-BSP NPs did not only have multiple sites of absorption in the gastrointestinal tract to guarantee their full utilization but also improved the absorption of OME in the stomach. Due to the degradation in the acidic environment, free OME was mainly absorbed in the intestine (Figure 3C and D) and distributed into the bloodstream. This promotes a delayed release and, consequently, a delayed absorption.[62] However, due to the improvement of OME stability and absorption in the stomach from OME-BSP NPs, OME from OME-BSP NPs treated rat gastric ulcer quicker and better. As a result, the combination of OME and BSP nanopreparations has a better synergistic antigastric ulcer effect, as shown in Figure 8.

In summary, our formulation reduces the metabolic rate of OME in the blood and stomach by protecting OME from complex biological environments such as pH. As nanoparticles degraded, OME was gradually released into the environment, resulting in sustained plasma concentrations and effective absorption levels in the stomach. Finally, by combining OME with BSP in the nanospheres, OME-BSP NPs can effectively and synergistically treat the rat gastric ulcer. The pharmacodynamic improvement of OME and targeted treatment was achieved.

5. CONCLUSIONS

In this study, we fabricated a nanosphere formulation loaded with OME and BSP, suitable for people with bleeding gastric ulcers. The prepared OME-BSP NPs were spherical, uniformly dispersed, small in size, and with good drug loading. OME-BSP NPs were mucoadhesive and stable, which can be trapped in the folds of the stomach, leading to the prolonged residence time and the increase of absorption. The pharmacodynamic improvement of OME and targeted therapy was achieved. Ultimately, the local or systemic effects of OME were realized, and its dual-use characteristics were fully enabled. Therefore, it can be safely concluded that OME-BSP NPs were effective and had potential in the treatment of gastric ulcer.

AUTHOR INFORMATION

Corresponding Author

Chang Yang − *State Key Laboratory of Functions and Applications of Medicinal Plants/Guizhou Provincial Key Laboratory of Pharmaceutics, Guizhou Medical University, Guiyang 550004 Guizhou, China; Engineering Research Center for the Development and Application of Ethnic Medicine and TCM (Ministry of Education), Guizhou Medical University, Guiyang 550004 Guizhou, China;* orcid.org/0000-0002-3986-8160; Email: yangchang@gmc.edu.cn

Authors

Lisu Li − *State Key Laboratory of Functions and Applications of Medicinal Plants/Guizhou Provincial Key Laboratory of Pharmaceutics, Guizhou Medical University, Guiyang 550004 Guizhou, China; School of Pharmacy, Guizhou Medical University, Guiyang 550004 Guizhou, China*

Jincheng Jing − *State Key Laboratory of Functions and Applications of Medicinal Plants/Guizhou Provincial Key Laboratory of Pharmaceutics, Guizhou Medical University, Guiyang 550004 Guizhou, China; School of Pharmacy, Guizhou Medical University, Guiyang 550004 Guizhou, China*

Shanshan Yang − *State Key Laboratory of Functions and Applications of Medicinal Plants/Guizhou Provincial Key Laboratory of Pharmaceutics, Guizhou Medical University, Guiyang 550004 Guizhou, China; School of Pharmacy, Guizhou Medical University, Guiyang 550004 Guizhou, China*

Shumei Fang − *State Key Laboratory of Functions and Applications of Medicinal Plants/Guizhou Provincial Key Laboratory of Pharmaceutics, Guizhou Medical University, Guiyang 550004 Guizhou, China; School of Pharmacy, Guizhou Medical University, Guiyang 550004 Guizhou, China*

https://doi.org/10.1021/acs.molpharmaceut.2c00922
Mol. Pharmaceutics XXXX, XXX, XXX−XXX

Wenting Liu − *State Key Laboratory of Functions and Applications of Medicinal Plants/Guizhou Provincial Key Laboratory of Pharmaceutics, Guizhou Medical University, Guiyang 550004 Guizhou, China; School of Pharmacy, Guizhou Medical University, Guiyang 550004 Guizhou, China*

Cong Wang − *State Key Laboratory of Functions and Applications of Medicinal Plants/Guizhou Provincial Key Laboratory of Pharmaceutics, Guizhou Medical University, Guiyang 550004 Guizhou, China; School of Pharmacy, Guizhou Medical University, Guiyang 550004 Guizhou, China*

Ruixi Li − *State Key Laboratory of Functions and Applications of Medicinal Plants/Guizhou Provincial Key Laboratory of Pharmaceutics, Guizhou Medical University, Guiyang 550004 Guizhou, China; Engineering Research Center for the Development and Application of Ethnic Medicine and TCM (Ministry of Education), Guizhou Medical University, Guiyang 550004 Guizhou, China*

Ting Liu − *State Key Laboratory of Functions and Applications of Medicinal Plants/Guizhou Provincial Key Laboratory of Pharmaceutics, Guizhou Medical University, Guiyang 550004 Guizhou, China; Engineering Research Center for the Development and Application of Ethnic Medicine and TCM (Ministry of Education), Guizhou Medical University, Guiyang 550004 Guizhou, China*

Lin Zheng − *State Key Laboratory of Functions and Applications of Medicinal Plants/Guizhou Provincial Key Laboratory of Pharmaceutics, Guizhou Medical University, Guiyang 550004 Guizhou, China; Engineering Research Center for the Development and Application of Ethnic Medicine and TCM (Ministry of Education), Guizhou Medical University, Guiyang 550004 Guizhou, China*

Complete contact information is available at: https://pubs.acs.org/10.1021/acs.molpharmaceut.2c00922

Author Contributions

[‖]L.L. and J.J. contributed equally to this work. L.L.: Methodology, software, investigation, writing—original draft; J.J.: Software, investigation; S.Y.: Software, investigation; Visualization, investigation; S.F.: Investigation; W.L.: Methodology, investigation; C.W.: Methodology, software; R.L.: Visualization; T.L.: Visualization; Z.L.: Visualization; C.Y.: Conceptualization, supervision, writing—reviewing and editing, and funding acquisition.

Funding

This work was supported by the National Natural Science Foundation of China-Guizhou Joint Fund [U1812403-5] and Cultivate project of Guizhou Medical University for National Natural Science Foundation [20NSP071].

Notes

The authors declare no competing financial interest.

The authors declare that they have no known competing financial interests or personal relationships that could have appeared to influence the work reported in this paper.

REFERENCES

(1) Al-Wajeeh, N. S.; Hajrezaie, M.; Al-Henhena, N.; Kamran, S.; Bagheri, E.; Zahedifard, M.; Saremi, K.; Noor, S. M.; Ali, H. M.; Abdulla, M. A. The antiulcer effect of *Cibotium barometz* leaves in rats with experimentally induced acute gastric ulcer. *Drug Des. Dev. Ther.* **2017**, *11*, 995−1009.

(2) Graham, D. Y. History of Helicobacter pylori, duodenal ulcer, gastric ulcer and gastric cancer. *World J. Gastroenterol.* **2014**, *20*, 5191−5204.

(3) Maity, P.; Biswas, K.; Roy, S.; Banerjee, R. K.; Bandyopadhyay, U. Smoking and the pathogenesis of gastroduodenal ulcer–recent mechanistic update. *Mol. Cell. Biochem.* **2003**, *253*, 329−338.

(4) Bagnardi, V.; Rota, M.; Botteri, E.; Tramacere, I.; Islami, F.; Fedirko, V.; Scotti, L.; Jenab, M.; Turati, F.; Pasquali, E.; Pelucchi, C.; Galeone, C.; Bellocco, R.; Negri, E.; Corrao, G.; Boffetta, P.; La Vecchia, C. Alcohol consumption and site-specific cancer risk: a comprehensive dose-response meta-analysis. *Br. J. Cancer* **2015**, *112*, 580−593.

(5) Strate, L. L.; Singh, P.; Boylan, M. R.; Piawah, S.; Cao, Y.; Chan, A. T. A Prospective Study of Alcohol Consumption and Smoking and the Risk of Major Gastrointestinal Bleeding in Men. *PLoS One* **2016**, *11*, No. e0165278.

(6) Chuang, Y. S.; Wu, M. C.; Yu, F. J.; Wang, Y. K.; Lu, C. Y.; Wu, D. C.; Kuo, C. T.; Wu, M. T.; Wu, I. C. Effects of alcohol consumption, cigarette smoking, and betel quid chewing on upper digestive diseases: a large cross-sectional study and meta-analysis. *Oncotarget* **2017**, *8*, 78011−78022.

(7) Mahmoud, Y. I.; Abd El-Ghffar, E. A. Spirulina ameliorates aspirin-induced gastric ulcer in albino mice by alleviating oxidative stress and inflammation. *Biomed. Pharmacother.* **2019**, *109*, 314−321.

(8) Toljamo, K.; Niemelä, S.; Karvonen, A. L.; Karttunen, R.; Karttunen, T. J. Histopathology of gastric erosions. Association with etiological factors and chronicity. *Helicobacter* **2011**, *16*, 444−451.

(9) Mousa, A. M.; El-Sammad, N. M.; Hassan, S. K.; Madboli, A.; Hashim, A. N.; Moustafa, E. S.; Bakry, S. M.; Elsayed, E. A. Antiulcerogenic effect of Cuphea ignea extract against ethanol-induced gastric ulcer in rats. *BMC Complementary Altern. Med.* **2019**, *19*, No. 345.

(10) Wang, A.; Yerxa, J.; Agarwal, S.; Turner, M. C.; Schroder, V.; Youngwirth, L. M.; Lagoo-Deenadayalan, S.; Pappas, T. N. Surgical management of peptic ulcer disease. *Curr. Probl. Surg.* **2020**, *57*, No. 100728.

(11) Bi, W. P.; Man, H. B.; Man, M. Q. Efficacy and safety of herbal medicines in treating gastric ulcer: a review. *World J. Gastroenterol.* **2014**, *20*, 17020−17028.

(12) Saranya, P.; Geetha, A.; Selvamathy, S. M. A biochemical study on the gastroprotective effect of andrographolide in rats induced with gastric ulcer. *Indian J. Pharm. Sci.* **2011**, *73*, 550−557.

(13) Kim, G. H. Proton Pump Inhibitor-Related Gastric Mucosal Changes. *Gut Liver* **2021**, *15*, 646−652.

(14) Lanas, A.; Chan, F. K. L. Peptic ulcer disease. *Lancet* **2017**, *390*, 613−624.

(15) Chiba, N.; De Gara, C. J.; Wilkinson, J. M.; Hunt, R. H. Speed of healing and symptom relief in grade II to IV gastroesophageal reflux disease: a meta-analysis. *Gastroenterology* **1997**, *112*, 1798−1810.

(16) Strand, D. S.; Kim, D.; Peura, D. A. 25 Years of Proton Pump Inhibitors: A Comprehensive Review. *Gut Liver* **2017**, *11*, 27−37.

(17) Lopes-de-Campos, D.; Pereira-Leite, C.; Fontaine, P.; Coutinho, A.; Prieto, M.; Sarmento, B.; Jakobtorweihen, S.; Nunes, C.; Reis, S. Interface-Mediated Mechanism of Action-The Root of the Cytoprotective Effect of Immediate-Release Omeprazole. *J. Med. Chem.* **2021**, *64*, 5171−5184.

(18) Olbe, L.; Carlsson, E.; Lindberg, P. A proton-pump inhibitor expedition: the case histories of omeprazole and esomeprazole. *Nat. Rev. Drug Discovery* **2003**, *2*, 132−139.

(19) Koyyada, A. Long-term use of proton pump inhibitors as a risk factor for various adverse manifestations. *Therapies* **2021**, *76*, 13−21.

(20) He, X.; Wang, X.; Fang, J.; Zhao, Z.; Huang, L.; Guo, H.; Zheng, X. *Bletilla striata*: Medicinal uses, phytochemistry and pharmacological activities. *J. Ethnopharmacol.* **2017**, *195*, 20−38.

(21) Wu, Y.; Zhang, W.; Huang, J.; Luo, Z.; Li, J.; Wang, L.; Di, L. Mucoadhesive improvement of alginate microspheres as potential gastroretentive delivery carrier by blending with *Bletilla striata* polysaccharide. *Int. J. Biol. Macromol.* **2020**, *156*, 1191−1201.

(22) Liu, J. Y.; Wang, H. C.; Yin, Y.; Li, N.; Cai, P. L.; Yang, S. L. Controlled acetylation of water-soluble glucomannan from *Bletilla striata*. *Carbohydr. Polym.* **2012**, *89*, 158−162.
(23) Peng, Q.; Li, M.; Xue, F.; Liu, H. Structure and immunobiological activity of a new polysaccharide from *Bletilla striata*. *Carbohydr. Polym.* **2014**, *107*, 119−123.
(24) Wang, Y.; Han, S.; Li, R.; Cui, B.; Ma, X.; Qi, X.; Hou, Q.; Lin, M.; Bai, J.; Li, S. Structural characterization and immunological activity of polysaccharides from the tuber of *Bletilla striata*. *Int. J. Biol. Macromol.* **2019**, *122*, 628−635.
(25) Li, N.; Yang, X.; Liu, W.; Xi, G.; Wang, M.; Liang, B.; Ma, Z.; Feng, Y.; Chen, H.; Shi, C. Tannic Acid Cross-linked Polysaccharide-Based Multifunctional Hemostatic Microparticles for the Regulation of Rapid Wound Healing. *Macromol. Biosci.* **2018**, *18*, No. 1800209.
(26) Xi, G.; Liu, W.; Chen, M.; Li, Q.; Hao, X.; Wang, M.; Yang, X.; Feng, Y.; He, H.; Shi, C.; Li, W. Polysaccharide-Based Lotus Seedpod Surface-Like Porous Microsphere with Precise and Controllable Micromorphology for Ultrarapid Hemostasis. *ACS Appl. Mater. Interfaces* **2019**, *11*, 46558−46571.
(27) Song, J. W.; Seo, C. S.; Kim, T. I.; Moon, O. S.; Won, Y. S.; Son, H. Y.; Son, J. K.; Kwon, H. J. Protective Effects of Manassantin A against Ethanol-Induced Gastric Injury in Rats. *Biol. Pharm. Bull.* **2016**, *39*, 221−229.
(28) Jeon, W. Y.; Shin, I. S.; Shin, H. K.; Lee, M. Y. Gastroprotective effect of the traditional herbal medicine, Sipjeondaebo-tang water extract, against ethanol-induced gastric mucosal injury. *BMC Complementary Altern. Med.* **2014**, *14*, No. 373.
(29) Kapitonova, M.; Gupalo, S.; Alyautdin, R.; Ibrahim, I. A. A.; Salim, N.; Ahmad, A.; Talip, S. B.; Nwe, T. M.; Morokhina, S. Gastroprotective effect of Berberis vulgaris on ethanol-induced gastric mucosal injury: Histopathological evaluations. *Avicenna J. Phytomed.* **2022**, *12*, 30−41.
(30) Wang, L.; Yang, S.; Li, L.; Huang, Y.; Li, R.; Fang, S.; Jing, J.; Yang, C. A low-intensity repetitive transcranial magnetic stimulation coupled to magnetic nanoparticles loaded with scutellarin enhances brain protection against cerebral ischemia reperfusion injury. *J. Drug Delivery Sci. Technol.* **2022**, *74*, No. 103606.
(31) Zhang, C.; Gao, F.; Gan, S.; He, Y.; Chen, Z.; Liu, X.; Fu, C.; Qu, Y.; Zhang, J. Chemical characterization and gastroprotective effect of an isolated polysaccharide fraction from *Bletilla striata* against ethanol-induced acute gastric ulcer. *Food Chem. Toxicol.* **2019**, *131*, No. 110539.
(32) Jiang, Y.; Travagli, R. A. Hypothalamic-vagal oxytocinergic neurocircuitry modulates gastric emptying and motility following stress. *J. Physiol.* **2020**, *598*, 4941−4955.
(33) Rezazadeh, M.; Safaran, R.; Minaiyan, M.; Mostafavi, A. Preparation and characterization of Eudragit L 100-55/chitosan enteric nanoparticles containing omeprazole using general factorial design: in vitro/in vivo study. *Res. Pharm. Sci.* **2021**, *16*, 358−369.
(34) Amaral, G. P.; de Carvalho, N. R.; Barcelos, R. P.; Dobrachinski, F.; Portella Rde, L.; da Silva, M. H.; Lugokenski, T. H.; Dias, G. R.; da Luz, S. C.; Boligon, A. A.; Athayde, M. L.; Villetti, M. A.; Antunes Soares, F. A.; Fachinetto, R. Protective action of ethanolic extract of Rosmarinus officinalis L. in gastric ulcer prevention induced by ethanol in rats. *Food Chem. Toxicol.* **2013**, *55*, 48−55.
(35) Rios, E. R. V.; Rocha, N. F.; Venâncio, E. T.; Moura, B. A.; Feitosa, M. L.; Cerqueira, G. S.; Soares, P. M.; Woods, D. J.; de Sousa, F. C.; Leal, L. K.; Fonteles, M. M. Mechanisms involved in the gastroprotective activity of esculin on acute gastric lesions in mice. *Chem. Biol. Interact.* **2010**, *188*, 246−254.
(36) Ibrahim, M. F. G.; Allam, F. Potential stem cell-Conditioned medium and their derived exosomes versus omeprazole in treatment of experimental model of gastric ulcer. *Acta Histochem.* **2022**, *124*, No. 151896.
(37) Hristova, M.; Tzaneva, M.; Bekyarova, G.; Chivchibashi, D.; Stefanova, N.; Kiselova-Kaneva, Y. Molecular Mechanisms of Melatonin Protection from Gastric Mucosal Apoptotic Injury in Experimental Burns. *Molecules* **2018**, *23*, 749.
(38) Repetto, M. G.; Llesuy, S. F. Antioxidant properties of natural compounds used in popular medicine for gastric ulcers. *Braz. J. Med. Biol. Res.* **2002**, *35*, 523−534.
(39) Pan, J. S.; He, S. Z.; Xu, H. Z.; Zhan, X. J.; Yang, X. N.; Xiao, H. M.; Shi, H. X.; Ren, J. L. Oxidative stress disturbs energy metabolism of mitochondria in ethanol-induced gastric mucosa injury. *World J. Gastroenterol.* **2008**, *14*, 5857−5867.
(40) Marklund, S.; Marklund, G. Involvement of the superoxide anion radical in the autoxidation of pyrogallol and a convenient assay for superoxide dismutase. *Eur. J. Biochem.* **1974**, *47*, 469−474.
(41) Rudra, D. S.; Pal, U.; Chowdhury, N.; Maiti, N. C.; Bagchi, A.; Swarnakar, S. Omeprazole prevents stress induced gastric ulcer by direct inhibition of MMP-2/TIMP-3 interactions. *Free Radical Biol. Med.* **2022**, *181*, 221−234.
(42) Sidahmed, H. M.; Azizan, A. H.; Mohan, S.; Abdulla, M. A.; Abdelwahab, S. I.; Taha, M. M.; Hadi, A. H.; Ketuly, K. A.; Hashim, N. M.; Loke, M. F.; Vadivelu, J. Gastroprotective effect of desmosdumotin C isolated from Mitrella kentii against ethanol-induced gastric mucosal hemorrhage in rats: possible involvement of glutathione, heat-shock protein-70, sulfhydryl compounds, nitric oxide, and anti-Helicobacter pylori activity. *BMC Complementary Altern. Med.* **2013**, *13*, No. 183.
(43) Zhao, H.; Zhang, X.; Zhang, B.; Qu, X. Gastroprotective effects of diosgenin against HCl/ethanol-induced gastric mucosal injury through suppression of NF-$\kappa\beta$ and myeloperoxidase activities. *Open Life Sci.* **2021**, *16*, 719−727.
(44) Zou, Y.; Cui, X.; Xiang, Q.; Guo, M.; Liang, Y.; Qu, Y.; Yang, X. Protective effect of against ethanol-induced gastric ulcer and its mechanism. *J. Zhejiang Univ.* **2021**, *50*, 561−567.
(45) Park, H. S.; Seo, C. S.; Baek, E. B.; Rho, J. H.; Won, Y. S.; Kwun, H. J. Gastroprotective Effect of Myricetin on Ethanol-Induced Acute Gastric Injury in Rats. *J. Evidence-Based Complementary Altern. Med.* **2021**, *2021*, No. 9968112.
(46) Salas, M.; Ward, A.; Caro, J. Are proton pump inhibitors the first choice for acute treatment of gastric ulcers? A meta analysis of randomized clinical trials. *BMC Gastroenterol.* **2002**, *2*, No. 17.
(47) Ghumman, S. A.; Bashir, S.; Noreen, S.; Khan, A. M.; Riffat, S.; Abbas, M. Polymeric microspheres of okra mucilage and alginate for the controlled release of oxcarbazepine: In vitro &in vivo evaluation. *Int. J. Biol. Macromol.* **2018**, *111*, 1156−1165.
(48) Chen, Z.; Cheng, L.; He, Y.; Wei, X. Extraction, characterization, utilization as wound dressing and drug delivery of *Bletilla striata* polysaccharide: A review. *Int. J. Biol. Macromol.* **2018**, *120*, 2076−2085.
(49) Liao, Z.; Zeng, R.; Hu, L.; Maffucci, K. G.; Qu, Y. Polysaccharides from tubers of *Bletilla striata*: Physicochemical characterization, formulation of buccoadhesive wafers and preliminary study on treating oral ulcer. *Int. J. Biol. Macromol.* **2019**, *122*, 1035−1045.
(50) Maeng, J. H.; Bang, B. W.; Lee, E.; Kim, J.; Kim, H. G.; Lee, D. H.; Yang, S. G. Endoscopic application of EGF-chitosan hydrogel for precipitated healing of GI peptic ulcers and mucosectomy-induced ulcers. *J. Mater. Sci. Mater. Med.* **2014**, *25*, 573−582.
(51) Wang, Y.; Liu, J.; Li, Q.; Wang, Y.; Wang, C. Two natural glucomannan polymers, from Konjac and Bletilla, as bioactive materials for pharmaceutical applications. *Biotechnol. Lett.* **2015**, *37*, 1−8.
(52) Wang, L.; Wu, Y.; Li, J.; Qiao, H.; Di, L. Rheological and mucoadhesive properties of polysaccharide from *Bletilla striata* with potential use in pharmaceutics as bio-adhesive excipient. *Int. J. Biol. Macromol.* **2018**, *120*, 529−536.
(53) Tabata, Y. *New Polymer Materials*, Advances in Polymer Science; Springer Berlin: Heidelberg, 1990; Vol. *Chapter 4*, pp 107−141 DOI: 10.1007/BFb0043058.
(54) Lamprecht, A.; Schäfer, U.; Lehr, C. M. Size-dependent bioadhesion of micro- and nanoparticulate carriers to the inflamed colonic mucosa. *Pharm. Res.* **2001**, *18*, 788−793.
(55) Lamprecht, A.; Ubrich, N.; Yamamoto, H.; Schäfer, U.; Takeuchi, H.; Maincent, P.; Kawashima, Y.; Lehr, C. M.

Biodegradable nanoparticles for targeted drug delivery in treatment of inflammatory bowel disease. *J. Pharmacol. Exp. Ther.* **2001**, *299*, 775−781.
(56) Lamprecht, A.; Yamamoto, H.; Takeuchi, H.; Kawashima, Y. Nanoparticles enhance therapeutic efficiency by selectively increased local drug dose in experimental colitis in rats. *J. Pharmacol. Exp. Ther.* **2005**, *315*, 196−202.
(57) Ke, W.; Qiong, M. Clinical effect observation of Bletttila combine with omeprazole in the treatment of gastric ulcer. *J. Commun. Med.* **2019**, *17*, 1002−1004.
(58) Hasani, S.; Pellequer, Y.; Lamprecht, A. Selective adhesion of nanoparticles to inflamed tissue in gastric ulcers. *Pharm. Res.* **2009**, *26*, 1149−1154.
(59) Yue, L.; Wang, W.; Wang, Y.; Du, T.; Shen, W.; Tang, H.; Wang, Y.; Yin, H. *Bletilla striata* polysaccharide inhibits angiotensin II-induced ROS and inflammation via NOX4 and TLR2 pathways. *Int. J. Biol. Macromol.* **2016**, *89*, 376−388.
(60) Luo, L.; Zhou, Z.; Xue, J.; Wang, Y.; Zhang, J.; Cai, X.; Liu, Y.; Yang, F. *Bletilla striata* polysaccharide has a protective effect on intestinal epithelial barrier disruption in TAA-induced cirrhotic rats. *Exp. Ther. Med.* **2018**, *16*, 1715−1722.
(61) Gu, Q.; Liu, Y.; Zhen, L.; Zhao, T.; Luo, L.; Zhang, J.; Deng, T.; Wu, M.; Cheng, G.; Hu, J. The structures of two glucomannans from *Bletilla formosana* and their protective effect on inflammation via inhibiting NF-κB pathway. *Carbohydr. Polym.* **2022**, *292*, No. 119694.
(62) Castell, D. Review of immediate-release omeprazole for the treatment of gastric acid-related disorders. *Expert Opin. Pharmacother.* **2005**, *6*, 2501−2510.

https://doi.org/10.1021/acs.molpharmaceut.2c00922
Mol. Pharmaceutics XXXX, XXX, XXX−XXX